Metal palladium supported on amphiphilic microporous synthetic organic supports. Part II. Catalytic investigations

Milan Králik [a,*], Marco Zecca [b], Piero Bianchin [b], Angelo Antonio D'Archivio [c], Luciano Galantini [c], Benedetto Corain [c,d]

[a] *Department of Organic Technology, Slovak Technical University, Radlinského, SK-812 37 Bratislava, Slovak Republic*
[b] *Dipartimento di Chimica Inorganica, Metallorganica e Analitica, via Marzolo 1, 35131 Padua, Italy*
[c] *Dipartimento di Chimica, Università di L'Aquila, Ingegneria Chimica e Materiali, via Vetoio, 67010 L'Aquila, Italy*
[d] *Centro per lo Studio della Stabilita' e Reattivita' dei Composti di Coordinazione, C.N.R., via Marzolo 1, 35131 Padua, Italy*

Abstract

Two sets of resin-supported Pd(0) catalysts were compared in the hydrogenation of cyclohexene in methanol, under ambient conditions. Two lightly crosslinked poly-{styrene/2-methacryloxyethylsulfonic acid/methylenebisacrylamide} with different degrees of crosslinking (1 and 3 mol%), have been used as catalyst supports. Two catalysts with different palladium loadings (0.22 and 2.2 wt%) have been prepared from each support. When the size of the particles was relatively small, the catalysts with 2.2% and 0.22% Pd were almost equally active with respect to the amount of palladium in the reaction mixture. In contrast, when larger catalyst particles were used, catalysts with 2.2% metal produced conversion profiles typical of diffusion-controlled regimes (productivity decreased with increasing crosslinking). These catalysts were characterised by combined ESR and static gradient spin echo NMR spectrometries, which have provided information about molecular motion inside the polymer networks. © 1998 Elsevier Science B.V.

Keywords: Poly-{styrene-2-methacryloxyethylsulfonic acid-methylenebisacrylamide}; Palladium; Cyclohexene hydrogenation; Diffusive vs. kinetic regimes; ESR; Static gradient spin echo NMR

1. Introduction

A metal catalysis performed by polymer-supported polydispersed metal phases is an emerging section of the modern industrial chemical technology. The elegant one pot synthesis of methylisobutylketone from acetone and dihydrogen and the extremely efficient deoxygenation of water to be used in industrial heat exchangers [1–3] are two effective examples of the potentialities of this type of modern catalysts.

Macroporous matrices possess a permanent porosity both in the dry and wet state. They may be considered good candidate supports for metal catalysis, because the macropores are expected to allow the easy transport of reactant and product molecules to and from the metal crystallites found on the macropore surfaces [4–6]. However, organic microporous supports should also be carefully considered. They do

* Corresponding author. Tel.: +421-7-395242; fax: +421-7-393198; e-mail: kralik@checdek.chtf.stuba.sk

not possess a permanent porosity in the dry state, but they develop a tremendous 'surface area' [7], after swelling in convenient solvents. This can make them potentially suitable for an unrivalled degree of metal loading.
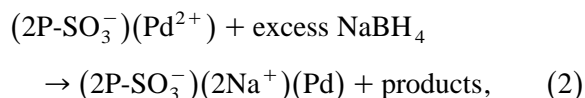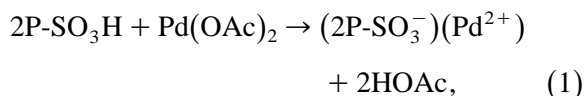
We have shown in our laboratories that nanoparticles (vide infra) of palladium can be easily and evenly dispersed throughout the bulk of properly designed microporous resins [8,9]. Moreover, we have also shown by means of inverse steric exclusion chromatography (ISEC) [10,11] that a large proportion of the gel phase volume of microporous resins based on N,N-dimethylacrylamide are accessible to molecules of a substantial size in a number of diverse swelling media [12,13]. In Part I of this series [14] we have shown that {styrene/2-methacryloxy-ethylsulfonic acid/methylenebisacrylamide} copolymers ($SO_3H = 1.4$ meq g^{-1}), with a degree of crosslinking ranging from 1 to 6 mol%, are amphiphilic in nature. In fact, they exhibit practically the same swellability (swelling volume) [14] in water as in tetrahydrofuran (THF). Not unexpectedly, they show a very marked compatibility with methanol, an amphiphilic solvent, as demonstrated by their bulk expanded volumes (BEV) [15], which are equal to 20.5 and 9.5 cm^3 g^{-1}, respectively, for the 1 and 3 mol% crosslinked materials. The XRM analysis performed on these catalysts revealed a homogeneous distribution of metal crystallites throughout the catalyst particles length (ca. 200 μm). Moreover, a distribution of the polymer chain concentration obtained from the ISEC measurements provided further fine information on morphology and textural properties. In particular, the effect of increasing crosslinking on the molecular mobility inside the polymer network can be quantified in terms of an increasing average polymer chain concentration (av.pcc) [10–13]. This is a valuable parameter as far as the nanoscopic morphology is concerned. The values of av.pcc in water were calculated as follows, from the data reported in Table 3, GV, and 4, L, in Ref. [14]: av. pcc = L/GV; where GV is the volume occupied by the gel phase and

L is the total length of polymer chain in the gel phase as respectively detected by ISEC. For the resins herein described, the average values of av.pcc observed in water are equal to 0.16 (1%) (P1Pd2) and 0.24 (3%) (P3Pd2) nm/nm^3.

In this paper the further characterisation of these two materials by ESR [12,13] and the static gradient spin echo NMR (SGSE-NMR) [16] spectrometries is reported. Furthermore, the catalytic activity of these resin/Pd(0) composites in the hydrogenation of cyclohexene is included. We also report the behaviour of catalysts prepared from the same supports (the same nanoscopic morphology), but with a lower loading (1/10) of the polydispersed metal catalytic phase. We show how the different metal loading strongly affects the catalytic regime, under otherwise identical conditions.

2. Experimental

All chemicals were of reagent grade. Cyclohexene was purified by distillation prior to use. The catalysts utilised in this work are coded as P1Pd2 (SS1MPd2 in Ref. [14]), P1Pd02, P3Pd2 (SS3MPd2 in Ref. [14]) and P3Pd02. The former two are based on a 1 mol% crosslinked support and the latter two on a 3 mol% crosslinked support. P1Pd02 and P3Pd02 were obtained exactly as were the catalysts described previously according to

$$2P\text{-}SO_3H + Pd(OAc)_2 \rightarrow (2P\text{-}SO_3^-)(Pd^{2+})$$
$$+ 2HOAc, \quad (1)$$

$$(2P\text{-}SO_3^-)(Pd^{2+}) + \text{excess } NaBH_4$$
$$\rightarrow (2P\text{-}SO_3^-)(2Na^+)(Pd) + \text{products}, \quad (2)$$

where P denotes a polymeric backbone. The amount of Pd(OAc)$_2$ employed ensured that the desired metal percentage in the catalysts was achieved. The excess of NaBH$_4$ allowed both the reduction of Pd(II) to Pd(0) and the full substitution of H$^+$ by Na$^+$.

ESR spectra were recorded on a JEOL JES-RE1X apparatus. About 0.25 g of material were swollen with a 10^{-4} M solution of TEMPONE (2,2,6,6-tetramethyl-4-oxo-1-oxyl-piperidine) in methanol, saturated with nitrogen. The samples were allowed to stand in the solution for about 2 h. After the removal of the solution by filtration, the swollen samples were placed inside the ESR tube and the spectra were recorded at ca. 298 K.

SGSE-NMR spectra were recorded on a Bruker SXP 4-100 MHz apparatus. The materials were allowed to swell in the minimum amount of methanol and then treated as described just above. The spin–echo was registered at ca. 298 K. The amplitude of the signal was measured at the constant pulse time 10 ms by varying magnetic field gradient from 0 to 21.4 G cm^{-1}.

2.1. 'Palladinising' of resins in the acid form with palladium acetate

Typically 1 g of resin (ca. 1.4 mmol of SO_3H functional groups) was swollen in a methanol–acetone mixture (1:1, vol/vol) and the excess solvent was removed after 4 h upon decantation. The swollen resin was mixed with 5 cm^3 of a dark brown solution of $Pd(OAc)_2$ (4.3×10^{-3} M, methanol–acetone 1:1, vol/vol), under vigorous stirring. The fast decolouration of the solution was observed and, at the same time, the colour of the resin turned from white to a very dark brown. The ion-exchange process was let to proceed for 3 h. The exchanged resin was washed with methanol (3×30 cm^3) and then dried in vacuo to constant weight (mechanical oil pump, $P =$ ca. 10 Pa, room temperature).

2.2. Reduction of Pd(II) to Pd(0) in the exchanged resins

Typically 1.0 g of the Pd(II)-exchanged resin (0.021 mmol of metal) was swollen in the minimum amount of ethanol. After standing for 4 h, it was quickly mixed with a solution of $NaBH_4$ in ethanol (6.6×10^{-2} M, 25.6 cm^3, 1.69 mmol), under vigorous stirring. After 2 h the black material was filtered, washed with ethanol (3×30 cm^3) and dried in vacuo to a constant weight (mechanical oil pump, $P =$ ca. 10 Pa, room temperature). The dry powder catalyst was sieved and three fractions were obtained having diameter ranges of 1–0.3, 0.3–0.1 and less than 0.1 mm. Fractions of P1Pd2 and P3Pd2 catalysts [14] were separated by sieving as well.

2.3. Catalytic tests

Catalytic experiments were carried out in a 50 cm^3 glass-lined stainless steel reactor, connected with a flexible metal capillary to an apparatus for measuring the hydrogen consumption at a constant pressure [17].

Experiments were performed at 25°C and 0.5 MPa. In all cases, 10 cm^3 of a 1 M solution of cyclohexene in methanol were employed, with an amount of the catalyst yielding a palladium amount per unit volume of the reaction mixture [Pd] 2.5×10^{-4} mol m^{-3}. The reactor was filled with reactants, the catalyst and hydrogen, then immersed in an oil bath and vigorously shaken at a frequency of 6 Hz. Catalyst recycling tests were performed after filtration and washing by methanol under hydrogen and reloading the autoclave with the catalyst under hydrogen.

3. Results and discussion

In our previous paper [14], we showed that uniform distributions of metal palladium in catalysts P1Pd2 and P3Pd2 could be easily achieved under the reduction conditions herein described. Owing to the lower concentration of palladium in the catalysts P1Pd02 and P3Pd02, we could not detect the metal by XRMA as a means to observe its distribution in these materials. In Refs. [8,9], it has been shown that a tendency to obtain a uniform metal distribution increases with a decrease in palladium(II), and with a high concentration and large excess of the re-

ducing agent. Thus, in analogy with P1Pd2 and P3Pd2 [14], palladium is also expected uniformly dispersed in catalysts P1Pd02 and P3Pd02. Moreover, initial reaction rates measurements over the catalyst particles of different sizes demonstrated the uniform distribution of the metal crystallites throughout the catalyst particles indirectly.

On the basis of the preparation protocol, the sets of catalysts with 2.2 and 0.22 wt% palladium are expected to possess the same nanoscopic morphology [7,10,11] in a given swelling medium. This morphology can be assessed by means of ISEC as demonstrated in Ref. [14] for P1Pd2 and P3Pd2 catalysts swollen in water and tetrahydrofuran. Unfortunately, the direct ISEC analysis in methanol is often not reliable [18]. Therefore, the molecular accessibility of these polymer networks (and indirectly [12,13] their nanoscopic morphology) was also evaluated on the basis of the well known ESR and of the static gradient spin echo NMR (SGSE-NMR) [16] spectrometries in the same solvent used in the catalytic experiments.

In the SGSE-NMR technique, a liquid sample containing a set of magnetically active nuclei of the same type (for instance ^{1}H nuclei) is exposed to a fixed, homogeneous magnetic field. Then a second magnetic field is applied and finely varied according to a known linear gradient which results in a non-homogeneous magnetic field. The response of the nuclei (echo amplitude $A(\tau_p)$) after a pulse sequence $90° - \tau_p - 180° - \tau_p$ is quantitatively correlated to the self-diffusion coefficient of the molecules [16]. If the sample to be analysed is a liquid the experiments provide information on the translational mobility of the molecules of the liquid. If the sample is a swollen polymer, i.e. a liquid medium dispersed inside a microporous matrix, SGSE-NMR gives information on the translational mobility of the molecules of the liquid confined in the micropores of the polymeric material. The hydrogen nuclei from the polymer network relax very efficiently and therefore are not expected to interfere with the spin–echo
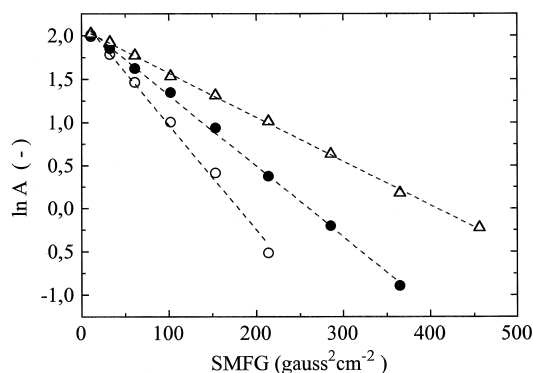

Fig. 1. SGSE-NMR measurements of self-diffusional coefficients. Logarithm of amplitude (ln *A*) vs. squared magnetic field gradient (SMFG); methanol in bulk (○), methanol in P1Pd2 (●) and in P3Pd2 (△).

signal of the liquid when proper duration of the pulse τ_p is chosen. Under these conditions, the height of the echo amplitude $A(\tau_p)$ is given by

$$A(\tau_p) = A_0 \exp\left(- \frac{2\tau_p}{T_2} - \tfrac{2}{3}\gamma^2 G^2 D \tau_p^3 \right), \qquad (3)$$

where T_2 is the spin–spin relaxation time (s), γ the magnetogyric ratio of ^{1}H (2.6737×10^4 rad s^{-1} G^{-1}), G the magnetic field gradient (G cm^{-1}) and D the self-diffusion coefficient (cm^2 s^{-1}).

The data obtained from SGSE-NMR measurements are given in Fig. 1. The solvent self-diffusion coefficient was calculated from the slope of the logarithmic plot of $A(\tau_p)$ vs. G^2.

Typical ESR spectra are depicted in Fig. 2, in which are also denoted parameters needful for the calculation of the rotational correlation time (τ) [19], i.e., $h(+1)$ and $h(-1)$ amplitudes of the low- and high-field spectral peaks, resp., and $\Delta h(+1)$ width of the low field spectral peak. The values of these parameters were determined by peak fitting. The calculation of τ was according to the formula [19]

$$\tau = 1.75 \times 10^{-9} \left(1 - \sqrt{\frac{h(-1)}{h(+1)}} \right) \Delta h(+1).$$
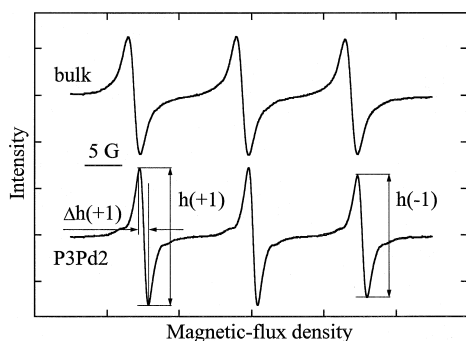
$$(4)$$

Fig. 2. Typical signals from ESR measurements; upper line: TEMPONE in bulk methanol, lower line: TEMPONE confined in the P3Pd2 swollen in methanol; $h(+1)$, $h(-1)$, $\Delta h(+1)$: quantities for Eq. (4). The line titled 5G represents magnetic-flux density 5 G.

The ESR and SGSE-NMR results are collected in Table 1.

In order to evaluate the consistency of the results obtained by the ESR method, SGSE-NMR method and predictability of the molecules' mobility on the basis of av.pcc and swellability, it is worthwhile to discuss the behaviour of molecules of different type confined in a swollen polymer.

(i) The amphiphilic nature of the investigated materials was fairly well demonstrated by a relatively good swellability in water (hydrophilic agent) and THF (hydrophobic agent). Slightly higher swellability in water in comparison to THF and the chemical structure of the materials (the higher molar content of hydrophobic moieties than hydrophilic ones) indicated that water is a better swelling agent for the hydrophilic fraction of the polymer networks than THF is for the hydrophobic ones. The BEV values observed in methanol for our catalysts are approximately 3–5 times larger than those observed both in water and THF (Table 1). This large swelling volume may be explained by the amphiphilic character of the polymer and the high affinity of methanol to both hydrophilic and hydrophobic domains. For example, the polymer chain length of P3Pd2 material was 4.6×10^8 and 19.7×10^8 km g^{-1}, in water and THF, resp. [14]. If the swelling

power of methanol is assumed to be the same for both the hydrophilic and the hydrophobic fractions of the polymer networks and close to the swelling ability of water for the hydrophilic parts of the polymeric materials, the swellability of these materials in methanol should be 4–6 times larger than in water or THF. This prediction is in accordance with experimental observation (Table 1). The assumption of the same methanol–polymer affinity as is the affinity of water to hydrophilic domains of the polymer network enables us to consider the same ratios of av. pcc measured for different polymers: those swollen in water and those swollen in methanol.

(ii) The precise value of swellability (the volume which is truly occupied by the swollen polymer mass) can only be measured by means of ISEC [10,11]. Due to an enthalpic polymer–methanol interaction [18], values of swellability in methanol are not available and, we could mainly take into account BEV quantities (BEV

Table 1
Swellability (S), bulk expanded volume (BEV), polymer chain concentration (av.pcc) [10,11], rotational mobility (τ) [12,13], translational mobility (D) [16] and derived quantities for catalysts P1Pd2 and P3Pd2

Item	Catalyst	
	P1Pd2	P3Pd2
S-ISEC-water[a] (cm^3 g^{-1})	2.72	1.89
BEV-water (cm^3 g^{-1})	4.1	2.2
BEV-THF (cm^3 g^{-1})	6.3	3.9
BEV-MeOH (cm^3 g^{-1})	20.5	9.5
av.pcc-water[a] (nm nm^{-3})	0.16	0.24
τ-MeOH[b] (ps)	60 ± 17	115 ± 18
$D^c \times 10^{+5}$ (cm^2 s^{-1})	1.8 ± 0.2	1.1 ± 0.15
τ / τ_0 ($\tau_0 = 37 \pm 17$)[d]	1.6	3.1
D_0 / D ($D_0 = 2.5 \pm 0.3$)[d]	1.4	2.3

Errors in measured values were calculated on the basis of repeated measurements (5 or 6) using the standard procedure (see e.g. [23]) for the 95% probability level.
[a] Swellability and average polymer chain concentration determined in water [14].
[b] Rotational correlation time of TEMPONE dissolved in methanol confined inside the microporous network of the catalysts.
[c] Diffusion coefficient of methanol inside the microporous network of the catalysts.
[d] Values for bulk methanol, units are the same as for quantities in the swollen catalyst.

also includes the volume of the void spaces among the swollen polymer particles). The following values of ratios of BEV and ratios of S values for P1Pd2 and P3Pd2 catalysts (Table 1) were calculated (subscripts 1 and 2 denote P1Pd2 and P3Pd2 catalysts, resp.):

$S_1:S_2$

$= 1.45, \qquad (\text{BEV-water})_1:(\text{BEV-water})_2$

$= 1.86, \qquad (\text{BEV-THF})_1:(\text{BEV-THF})_2$

$= 1.61, \qquad (\text{BEV-MeOH})_1:(\text{BEV-MeOH})_2$

$= 2.15.$

A discrepancy in the S ratio and the BEV-MeOH ratio should be again explained by a strong methanol–polymer interaction, which results in a large solvation of polymeric chains. Due to this solvation, the polymer tends to swell, but the crosslinking limits the process. Therefore, the methanol–polymer interaction is more evident for the lower crosslinked material, and this causes the highest ratio of BEVs in methanol in comparison with BEVs in THF and water.

(iii) If a swollen microporous polymer is considered as a homogeneous medium, the viscosity of this medium increases with decreasing swellability of the polymer [12,13]. A viscosity dependence of both the translational and rotational diffusion may be expressed by the Stokes–Einstein relationship [20], but this holds only in the case of Brownian solutes. When the affinity of TEMPONE to the polymeric chains is supposed much lower than that of methanol the interaction TEMPONE–polymer should be practically negligible in the low concentrated TEMPONE's solution in methanol. The polymeric chains are likely to be completely solvated mainly by methanol molecules. Hence, a pure 'Stokes' behaviour of TEMPONE can be observed when the viscosity of the medium varies. In contrast, appreciable enthalpic interactions between methanol and the polymer back-

bone (this is the reason why an ISEC analysis in this liquid could not be carried out reliably) raise the question of whether methanol can be considered as a Brownian solute in our systems. The existence of this interference makes the rotational correlation time of TEMPONE the more reliable quantity than the self-diffusion coefficient of methanol.

Keeping in mind the problems mentioned, we made comparison in quantities obtained by different techniques. The following relationships were exploited in our previous work [21] to describe relationships among swellability, rotational mobility and translational mobility:

$$\ln(\tau/\tau_0) = a/S \qquad (5)$$

and

$$\ln(D/D_0) = -b/S, \qquad (6)$$

where a and b are adjustable parameters. The values of parameters a and b seem to be close to each other [21], ranging from 3 to 5, when S is given in cm^3/g. If a and b are assumed to have the same value, then

$$\tau/\tau_0 = D_0/D \qquad (7)$$

and

$$\tau_2/\tau_1 = D_1/D_2, \qquad (8)$$

where the subscripts 1 and 2 denote values for the material 1 and 2 respectively.

The data reported in Table 1 demonstrate that Eq. (7) apparently holds for the P1Pd2 catalyst ($\tau/\tau_0 = 1.6$; $D_0/D = 1.4$). A higher discrepancy between the values of these two ratios was observed (3.1 vs 2.3) for the P3Pd2 catalyst. Values of the rotational correlation time are referred to the TEMPONE in methanol and the diffusional coefficients are referred to the methanol itself (self-diffusion). In spite of the problems discussed above, quite consistent values were obtained for terms in Eq. (8) and the ratio of av.pcc (the subscripts 1 and 2 refer to P1Pd2 and P3Pd2, resp.),

$(\text{av.pcc})_2/(\text{av.pcc})_1 = 1.5,$

$(\tau_2/\tau_1) = 1.91,$

$(D_1/D_2) = 1.63.$

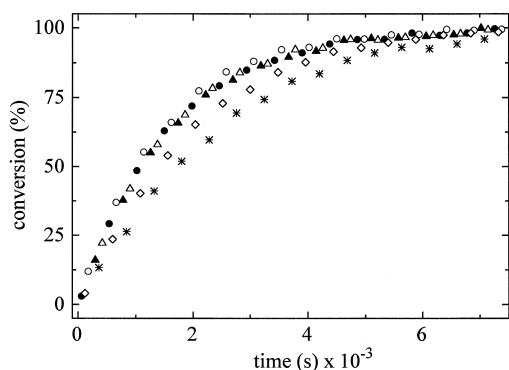Fig. 3. Kinetic plots for the hydrogenation of cyclohexene catalysed by P1Pd02 and P3Pd02 materials. Symbols are explained in Table 2.

Table 2
The initial rate (ξ_V) vs. the particle size (d) in the hydrogenation of cyclohexene over polymer catalysts charged by 0.22 wt% of palladium

Catalyst	d (mm)	$\xi_V \times 10^5$ (mol dm^{-3} s^{-1})	Relevant symbol in Fig. 3
P1Pd02	< 0.1	64	●
P3Pd02	< 0.1	70	○
P1Pd02[a]	< 0.1	59	not involved
P3Pd02[a]	< 0.1	74	not involved
P1Pd02	0.1–0.3	63	▲
P3Pd02	0.1–0.3	62	△
P1Pd02	0.3–0.7	52	◇
P3Pd02	0.3–0.7	43	∗

[a] The next sets of catalysts prepared from original resins.

So, it can be concluded that all the three methods (ISEC, SGSE-NMR and ESR) give a comparable evaluation of the mobility differences inside a microporous swollen polymer. It is worthwhile to add that both correlation time and diffusional coefficient depend on av.pcc exponentially; therefore, the ratios given above need to be considered as a qualitative comparison.

The catalysts P1Pd2, P3Pd2, P1Pd02, P3Pd02 were employed in the hydrogenation of cyclohexene in methanol at ambient conditions. The two sets of catalysts have been tested and compared under the conditions described in the experimental section. In all tests the conversion of cyclohexane to cyclohexene was quantitative. The catalysts could be recycled at least three times, without any measurable loss of activity, when the sizes of the catalyst particles were larger than 0.1 mm (dry state) and when the catalysts were filtered under hydrogen. Very fine catalyst particles, with sizes lower than 0.1 mm in the dry state, were not reusable and most solid was lost upon filtration and washing. The kinetic plots, obtained when different fractions of catalysts P1Pd02 and P3Pd02 were employed, are depicted in Fig. 3. From the shape of the conversion vs. time plots the reaction appears to occur under the true kinetic regime. Thus, initial reaction rates (Table 2) are independent of the translational mobility of the chemical species involved, in that they refer to catalyst particles of different sizes. Under these conditions the lower palladium content in each catalyst particle (i.e. in each 'microreactor') implies a reduction of the intrinsic reaction rate. Therefore, the expected increase of the diffusional resistance to the transport of matter inside the catalysts with increasing values of their av. pcc is not kinetically limiting. The diffusional resistance starts to be significant for particles larger than 0.3 mm and in this case the effect of the increasing crosslinking degree (i.e. av. pcc) is evident.

The results from the catalytic tests of materials containing 2.2% of metallic palladium are illustrated in Fig. 4 and Table 3. It is assumed that the kinetic regime is achieved only when very small (less than 0.1 mm) particles of the
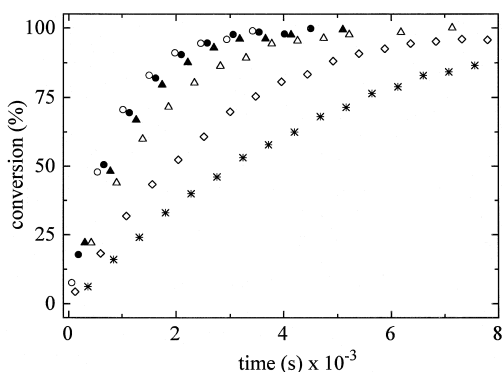

Fig. 4. Kinetic plots for the hydrogenation of cyclohexene catalysed by P1Pd2 and P3Pd2 materials. Symbols are explained in Table 3.

Table 3
The initial rate (ξ_V) vs. the particle size (d) in the hydrogenation of cyclohexene over polymer catalysts charged by 2.2 wt% of palladium

Catalyst	d (mm)	$\xi_V \times 10^5$ (mol dm^{-3} s^{-1})	Relevant symbol in Fig. 4
P1Pd2	< 0.1	105	●
P3Pd2	< 0.1	111	○
P1Pd2[a]	< 0.1	97	not involved
P3Pd2[a]	< 0.1	105	not involved
PdPd2	0.1–0.3	89	▲
P3Pd2	0.1–0.3	67	△
P1Pd2	0.3–0.7	40	◇
P3Pd2	0.3–0.7	24	*

[a]The next sets of catalysts prepared from original resins.

catalyst are employed. The hindrance of the rate due to the diffusion of reactants increases rapidly with increasing the catalyst particle size. The shape of the conversion vs. time for experiments with the largest particles (larger than 0.3 mm) suggests clearly that the diffusion controlled regime has been obtained. Expectedly, the reaction is faster for the less crosslinked matrix due to the lower diffusional resistance. The lower diffusional resistance is also featured by the lower av.pcc, higher S and BEV, as well as, by ESR and SGSE-NMR data (Table 1).

The values of the initial reaction rate observed over small catalyst particles are significantly different for all the tested catalysts. When the percentage of palladium is relatively high (2.2 wt%), the activity is remarkably higher (initial rates: 105 and 111×10^{-5} mol dm^{-3} s^{-1} for the P1Pd2 and P3Pd2, respectively) than in the case of catalysts with a low metal load (0.22 wt%, initial rates: 64 and 70×10^{-5} mol dm^{-3} s^{-1} for the P1Pd02 and P3Pd02, respectively). To confirm this finding, all catalysts were prepared once more and catalytic tests with the smallest particles were repeated. The values of initial rates obtained with this second set of catalysts were comparable with those reported in Tables 2 and 3. This proved that the molar specific activity of palladium crystallites dispersed into a polymeric support depends on the percentage loading of palladium in the catalyst. Probably, an optimal value of palladium

load exists, and finding out this maximum should be of interest. On the other hand, catalysts containing more palladium than, e.g., 1 wt% are not of great practical interest, due to the diffusional resistance when larger catalyst particles are used. Therefore, the optimization of the molar specific activity of palladium is important only from the theoretical point of view.

4. Conclusions

Pd catalysts were made up from amphiphilic resins featured by the 0.16 and 0.24 nm nm^{-3} polymer chain concentration. The catalysts exhibited a kinetic behaviour dependent on the textural properties, metal load and catalysts particle size. For 0.2 wt% metal loading a true kinetic regime was observed for catalysts particles ranging from 0.1 to 0.3 mm, while a diffusion control was observed for 2.2 wt% metal loadings. In the latter catalysts productivity increased with the decreased polymer chain concentration.

The instrumental technique SGSE-NMR was tested. It complements procedures used before (XRMA, ISEC, ESR, X-ray powder diffraction) [8,9]. All these methods allow the achievement of a wide spectrum of information and can help in tailoring new polymer supported metal catalysts, as well as in analysing problems occurring during the exploitation of common polymeric catalysts.

The results presented herein act in favour of a wider utilisation of crosslinked polymer networks in metal catalysis. The rather common belief that metal crystallites dispersed into polymeric supports are 'buried' in an essentially impenetrable maze of polymer chains is just a bias. The diffusion resistance due to the support nature can be suppressed under the proper tailoring of a catalyst and operating conditions (lipophilic properties of the support, crosslinking degree, catalyst particle size, loading of metal, pressure, temperature, etc.). The diffusional resistance may also be useful in some

cases. A polymer-supported metal catalyst with a controlled nanoscopic morphology could be designed to allow a controlled diffusion of molecules throughout the catalyst particles. Under such a controlled diffusional regime, the polymer network acts as a 'molecular sieve' similar to the action of zeolite catalysts, with the advantage of wider and easier routes to the functionalisation and the metal loading of the solid materials.

Finally, the polymer network could, for instance, chemically interact with the reagents and, or the products. This feature is important for a multifunctional catalysis [22].

Acknowledgements

References

[1] R. Wagner, P.M. Lange, Erdöl Erdgas Kohle 105 (1989) 414.
[2] BAYER-Information LEWATIT-LEWASORB: Kationenaustascher als Katalysatoren, 1985.
[3] H. Widdecke, in: D.C. Sherrington, P. Hodge (Eds.), Synthesis and separations using functional polymers, Wiley, New York, 1988, p. 149.
[4] A. Guyot, in: D.C. Sherrington, P. Hodge (Eds.), Synthesis and separations using functional polymers, Wiley, New York, 1988, p. 1.
[5] A. Guyot, Pure Appl. Chem. 60 (1988) 365.
[6] R. Albright, Reactive Polymers 4 (1986) 155.
[7] B. Corain, K. Jeřábek, Chim. Ind. Milan 78 (1996) 563.
[8] M. Králik, M. Hronec, S. Lora, G. Palma, M. Zecca, A. Biffis, B. Corain, J. Mol. Catal. A: Chemical 97 (1995) 145.
[9] M. Králik, M. Hronec, S. Lora, G. Palma, M. Zecca, A. Biffis, B. Corain, J. Mol. Catal. A: Chemical 101 (1995) 143.
[10] K. Jeřábek, Anal. Chem. 57 (1985) 1595.
[11] K. Jeřábek, Anal. Chem. 57 (1985) 1598.
[12] A. Biffis, B. Corain, M. Zecca, C. Corvaja, K. Jerábek, J. Am. Chem. Soc. 117 (1995) 1603.
[13] M. Zecca, A. Biffis, G. Palma, C. Corvaja, S. Lora, K. Jeřábek, B. Corain, Macromolecules 29 (1996) 4655.
[14] M. Zecca, M. Králik, M. Boaro, G. Palma, S. Lora, M. Zancato, B. Corain, J. Mol. Catal., submitted.
[15] R. Arshady, Adv. Mater. 3 (1991) 182.
[16] S.K. Ghosh, E. Tettamanti, A. Ricchiuto, Chem. Phys. Lett. 101 (1983) 499, and references therein.
[17] M. Hronec, J. Ilavsky, Chem. Papers 39 (1985) 705.
[18] K. Jeřábek, unpublished results.
[19] P. Bailey, D.G. Gillies, L.H. Sutcliffe, J. Chem. Soc. Faraday Trans. 86 (1986) 3309.
[20] R.C. Reid, J.M. Prausnitz, B.E. Poling, The Properties of Gases and Liquids, 4th ed., Mc-Graw-Hill, New York, 1987.
[21] A. Biffis, B. Corain, Z. Cvengrošová, M. Hronec, K. Jeřábek, M. Králik, Appl. Catal. A: General 142 (1996) 327.
[22] B. Corain, M. Zecca, K. Jeřábek, Chem. Rev., submitted.
[23] D.C. Montgomery, G.C. Runger, Applied Statistics and Probability for Engineers, Wiley, New York, 1994.